

Evaluation of Diffuse Myocardial Fibrosis in Heart Failure With Cardiac Magnetic Resonance Contrast-Enhanced T_1 Mapping

Leah Iles, MBChB,* Heinz Pfluger, MD,* Arintaya Phrommintikul, MD,*
Joshi Cherayath, DIP AMIT,† Pelin Aksit, MS,‡ Sandeep N. Gupta, PhD,‡ David M. Kaye, PhD,*
Andrew J. Taylor, PhD*

Melbourne, Australia; and Bethesda, Maryland

- Objectives** The purpose of this study was to investigate a noninvasive method for quantifying diffuse myocardial fibrosis with cardiac magnetic resonance imaging (CMRI).
- Background** Diffuse myocardial fibrosis is a fundamental process in pathologic remodeling in cardiomyopathy and is postulated to cause increased cardiac stiffness and poor clinical outcomes. Although regional fibrosis is easily imaged with cardiac magnetic resonance, there is currently no noninvasive method for quantifying diffuse myocardial fibrosis.
- Methods** We performed CMRI on 45 subjects (25 patients with heart failure, 20 control patients), on a clinical 1.5-T CMRI scanner. A prototype T_1 mapping sequence was used to calculate the post-contrast myocardial T_1 time as an index of diffuse fibrosis; regional fibrosis was identified by delayed contrast enhancement. Regional and global systolic function was assessed by cine CMRI in standard short- and long-axis planes, with echocardiography used to evaluate diastology. An additional 9 subjects underwent CMRI and endomyocardial biopsy for histologic correlation.
- Results** Post-contrast myocardial T_1 times correlated histologically with fibrosis ($R = -0.7$, $p = 0.03$) and were shorter in heart failure subjects than controls (383 ± 17 ms vs. 564 ± 23 ms, $p < 0.0001$). The T_1 time of heart failure myocardium was shorter than that in controls even when excluding areas of regional fibrosis (429 ± 22 ms vs. 564 ± 23 ms, $p < 0.0001$). The post-contrast myocardial T_1 time shortened as diastolic function worsened (562 ± 24 ms in normal diastolic function vs. 423 ± 33 ms in impaired diastolic function vs. 368 ± 20 ms in restrictive function, $p < 0.001$).
- Conclusions** Contrast-enhanced CMRI T_1 mapping identifies changes in myocardial T_1 times in heart failure, which appear to reflect diffuse fibrosis. (J Am Coll Cardiol 2008;52:1574–80) © 2008 by the American College of Cardiology Foundation

Heart failure is a major cause of morbidity and mortality in the western world, causing over 1,000,000 hospitalizations/year in the U.S. (1). Although many advances have occurred in the medical management of systolic heart failure in the last 20 years, many patients ultimately progress to end-stage cardiomyopathy.

The heavy burden of heart failure necessitates further research into the basic pathophysiology of this growing epidemic. Recently, the importance of myocardial fibrosis in development and progression of systolic and diastolic cardiac failure has been highlighted (2,3). Myocardial fibrosis in animals is associated with worsening ventricular systolic

See page 1581

From the *Alfred Hospital and Baker IDI Heart and Diabetes Institute and †GE Healthcare, Melbourne, Australia; and the ‡Global Applied Science Laboratory, GE Healthcare, Bethesda, Maryland. Dr. Iles is supported by a National Health and Medical Research Council Post Graduate Research Scholarship, Melbourne, Australia. Dr. Pfluger is supported by a research grant from the Swiss National Science Foundation SNSF, Bern, Switzerland. Joshi Cherayath, Pelin Aksit, and Dr. Gupta are employees of GE Healthcare. Drs. Iles and Pfluger contributed equally to this work.

Manuscript received February 13, 2008; revised manuscript received May 8, 2008, accepted June 10, 2008.

function, abnormal cardiac remodeling, and increased ventricular stiffness (4). The link between collagen turnover and myocardial fibrosis is not fully understood, but it is thought to play an important role in the development of diastolic dysfunction (5,6). Also, increasing myocardial fibrosis results in progressive deterioration of myocardial function, with more

extensive myocardial fibrosis identified in patients with advanced heart failure, regardless of etiology of cardiomyopathy (7–9). A number of available therapies have been postulated to exert some of their beneficial effects via inhibition of myocardial fibrosis, principally through their actions on the renin-angiotensin-aldosterone system (10–13).

Regional myocardial fibrosis due to ischemic heart disease is well described with delayed contrast enhancement sequences on cardiac magnetic resonance imaging (CMRI) (14,15). Infarcted regions in the myocardium, having undergone scar formation with collagen deposition, have a much slower washout rate of gadolinium-based contrast than healthy myocardium, leading to a markedly increased signal intensity on T_1 -weighted imaging. A critical drawback to the technique of delayed contrast-enhanced CMRI in the detection of more diffuse myocardial fibrosis is that it is qualitative, not quantitative, and it relies on the difference in signal intensity between scarred and normal adjacent myocardium to generate image contrast. Because collagen deposition in nonischemic cardiomyopathy is commonly diffuse, the technique of delayed contrast enhancement often shows no regional scarring. A noninvasive test for myocardial fibrosis is highly desirable, not just in terms of disease stratification, but also in evaluating newer therapies aimed at reducing myocardial fibrosis in the treatment of heart failure.

Theoretically, diffusely fibrotic myocardium would accumulate contrast in a similar fashion to regional scarring, but calculation of the global T_1 time is required for its quantification. Studies in canine myocardium have identified alteration of the T_1 time with fibrosis (16), which correlated with myocardial collagen content. Similar findings have been demonstrated in hypertensive rat hearts (17) and in human papillary muscles (18).

In this prospective study we investigated the correlation between histologic fibrosis and myocardial post-contrast T_1 time. We also calculated the post-contrast T_1 time as an index of diffuse fibrosis in a group of heart failure subjects and controls and report an important mechanistic link between structural myocardial changes and functional impairment in heart failure.

Methods

Patient selection. All research was performed through the Alfred Hospital, Melbourne, Australia between March 2006 and December 2006. Subjects with heart failure of New York Heart Association functional class II or worse were invited to participate. **Subjects with normal left ventricular function and no symptoms of heart failure were recruited as a control group.** In all instances, subjects were excluded if they suffered from claustrophobia, uncontrolled atrial or ventricular tachyarrhythmias, or had a history of a metallic prosthetic implant contraindicating CMRI. Patients with recent myocardial infarction or myocarditis were

also excluded. No subject invited into either group declined to participate.

Endomyocardial biopsies and CMRI results were analyzed in an additional group of subjects with previous orthotopic heart transplantation. Subjects were excluded if they had acute rejection, were clinically unstable, or had a contraindication to CMRI. This group was not included in the overall analysis because 8 of the 9 subjects had preserved left ventricular systolic function, so were not suitable for inclusion in the heart failure group. Because they were not free of cardiac disease and would be expected to have a greater degree of myocardial fibrosis than a control population, they were also not appropriate for the control group.

Informed consent was obtained before CMRI for all participants, and the study was carried out under the guidelines of the Alfred Hospital Ethics Committee.

Histologic analysis. Transvenous right ventricular endomyocardial biopsy specimens from a separate group of subjects ($n = 9$) were fixed immediately in 10% buffered formalin, embedded in paraffin, routinely processed, and stained with picrosirius red to obtain contrast between myocardium and fibrotic areas. Three or four specimens were analyzed for each patient. Low-power enlargement was used to select appropriate areas for analysis, with exclusion of subendocardial or perivascular areas with high levels of collagen. Sites with marked scarring from previous biopsies were also excluded because these areas were regarded as nonrepresentative fields. Once the appropriate regions were selected, high-power magnification (200 \times) digital images were taken for all endomyocardial areas. Using an automated image analysis system (Optimas 6.51, Media Cybernetics, Bethesda, Maryland), we assessed collagen as a percentage of total endomyocardial area. Assessment of collagen by this morphometric approach has been shown to correlate well with myocardial levels of hydroxyproline (19).

CMRI protocol. MAGNETIC RESONANCE IMAGING SEQUENCES. We performed CMRI on 25 heart failure subjects, 20 control subjects, and 9 subjects with previous heart transplantation, on a clinical 1.5-T CMRI scanner (Signa HD 1.5-T, GE Healthcare, Waukesha, Wisconsin). All sequences were acquired during a breath-hold of 10 to 15 s. Left ventricular (LV) function was assessed by a **steady state free precession pulse sequence** (repetition time [TR] 3.8 ms, echo time [TE] 1.6 ms, 30 phases, **slice thickness 8 mm**).

Abbreviations and Acronyms

CCF = congestive cardiac failure
CMRI = cardiac magnetic resonance imaging
DE- = myocardium without delayed enhancement
DE+ = myocardium with delayed enhancement
ECG = electrocardiogram
GFR = glomerular filtration rate
ICMP = ischemic cardiomyopathy
IDCM = idiopathic dilated cardiomyopathy
LVEF = left ventricular ejection fraction
ROI = region of interest
TTE = transthoracic echocardiography

Delayed hyperenhancement was obtained 10 min after a bolus of gadolinium-diethylene triamine penta-acetic acid (DTPA) (0.2 mmol/kg BW Magnevist, Schering, Germany) to identify regional fibrosis using an inversion-recovery gradient echo technique (TR 7.1 ms, TE 3.1 ms, inversion time [TI] individually determined to null the myocardial signal, range 180 to 250 ms, slice thickness 8 mm, matrix 256×192 , number of acquisitions = 2).

For evaluation of diffuse fibrosis, a prototype sequence was used to cycle through acquisition of images over a range of inversion times. The sequence consisted of an electrocardiogram-triggered, inversion-recovery prepared, 2-dimensional fast gradient echo sequence employing variable temporal sampling of k-space (VAST) (20) (Global Applied Science Laboratory, GE Healthcare). Ten images were acquired sequentially at increasing inversion times (50 to 1,000 ms) 15 min after the bolus of gadolinium-DTPA mentioned earlier, typically over a series of 3 to 4 breath-holds. Imaging parameters were TR/TE: 3.7 ms/1.2 ms, flip angle: 20° , 256×128 acquisition matrix, 36×27 -cm field of view, 8-mm slice thickness, TI: 50 ms–1 s, trigger delay 300 ms, and views per segment 24. These images were then processed with a curve fitting technique to generate T_1 maps.

All cine CMRI sequences were performed in 3 standard short-axis slices (apical, mid, and basal), kept identical for each sequence throughout the CMRI examination (21). From an end-diastolic, 4-chamber, long-axis view, 5 equally spaced slices were planned, so that the 2 outer slices lined up exactly either with the tip of the apex or the mitral annulus. The 2 outer slices were then deleted, leaving 3 slices corresponding to typical basal, mid, and apical short-axis views. Delayed enhancement imaging was performed in both long- and short-axis views. For T_1 mapping, the middle slice short-axis slice was utilized.

Evaluation of LV function and regional fibrosis. LV function was evaluated globally using the biplane area-length method using 2- and 4-chamber long-axis views. Regional wall thickening was evaluated from the mid short axis view by calculating percent systolic thickening.

Regional fibrosis was identified by delayed enhancement within the myocardium, defined quantitatively by myocardial post-contrast signal intensity >2 SDs above that within a reference region of remote noninfarcted myocardium within the same slice.

Evaluation of diffuse fibrosis with T_1 mapping. Following image acquisition, the 10 short-axis images of varying inversion times were transferred to an external computer for analysis using a dedicated research software package (Cin-tool, Global Applied Science Laboratory, GE Healthcare). This provided the ability to analyze regions of interest (ROIs) to find average T_1 for that area, as well as a pixel-by-pixel determination of T_1 , by fitting data acquired at various preparation times to the exponential curve: $M_z(t = TI) = M_0(A - B[e^{-t/T_1}])$, relating the sample magnetization M_z observed at the time $t = TI$ to the equilibrium magnetization M_0 and sample T_1 , where TI denotes inversion

time for an inversion recovery experiment. For each image, an ROI was drawn around the entire myocardium to calculate post-contrast myocardial T_1 time for each subject (Fig. 1). In subjects with regional fibrosis detected by delayed enhancement, either due to infarction, mid-wall fibrosis from idiopathic dilated cardiomyopathy (IDCM), or patchy nonvascular distribution fibrosis from infiltrative cardiomyopathy, an additional analysis was performed in which regions of delayed enhancement were excluded from the ROI for calculation of post-contrast myocardial T_1 time. We also performed a third analysis in which the ROI was limited to only the region of myocardium with regional fibrosis on delayed enhancement imaging. For calculation of skeletal muscle T_1 time, the ROI was drawn around the pectoralis muscle.

Evaluation of diastolic function. Standard transthoracic echocardiography was performed as a baseline evaluation of cardiac morphology and function. Diastolic function was assessed by a combination of mitral flow inflow pattern (E to A ratio, deceleration time, and isovolumetric ventricular relaxation time), as well as mitral annular velocity (E'). In all cases an experienced cardiologist who was blinded to the CMRI findings graded diastolic function according to established guidelines (22,23). Diastolic function was expressed as either normal, impaired relaxation (including both delayed left ventricular relaxation and pseudo-normalization), or restrictive. Additionally, the mitral E/E' was calculated as an index of ventricular filling pressure.

Statistics. All data are expressed as mean \pm 1 standard error unless otherwise indicated. Comparison between groups using continuous variables utilized unpaired Student t test. Comparison between multiple groups was performed with analysis of variance (ANOVA), with post hoc analysis performed as appropriate. Pairwise multiple comparisons were performed using the Holm-Sidak method. Dependent variables were correlated by calculating the Pearson Product Moment. For all comparisons, a p value of <0.05 was considered significant.

Results

Clinical and demographic data. A total of 54 patients were evaluated in the study period. There were 25 patients with heart failure, 20 control subjects, and 9 heart transplant recipients (mean time after transplantation 1.7 ± 1.2 years) in whom histologic correlation of fibrosis with CMRI findings was obtained. Demographic data from the 45 heart failure and control subjects is presented in Table 1. Patients in the heart failure group were older, and there was a trend to an increased number of male subjects in the heart failure group (72% vs. 50%, $p = 0.13$, chi-square). There was no difference in heart rate between heart failure and control groups (mean heart rate 70 ± 3.4 beats/min vs. 67 ± 2.4 beats/min, $p = \text{NS}$), or in renal function (glomerular filtration rate 76.0 ± 13.6 ml/min/1.73 m^2 vs. 81.3 ± 12.1 ml/min/1.73 m^2 , $p = 0.71$). The heart failure group was

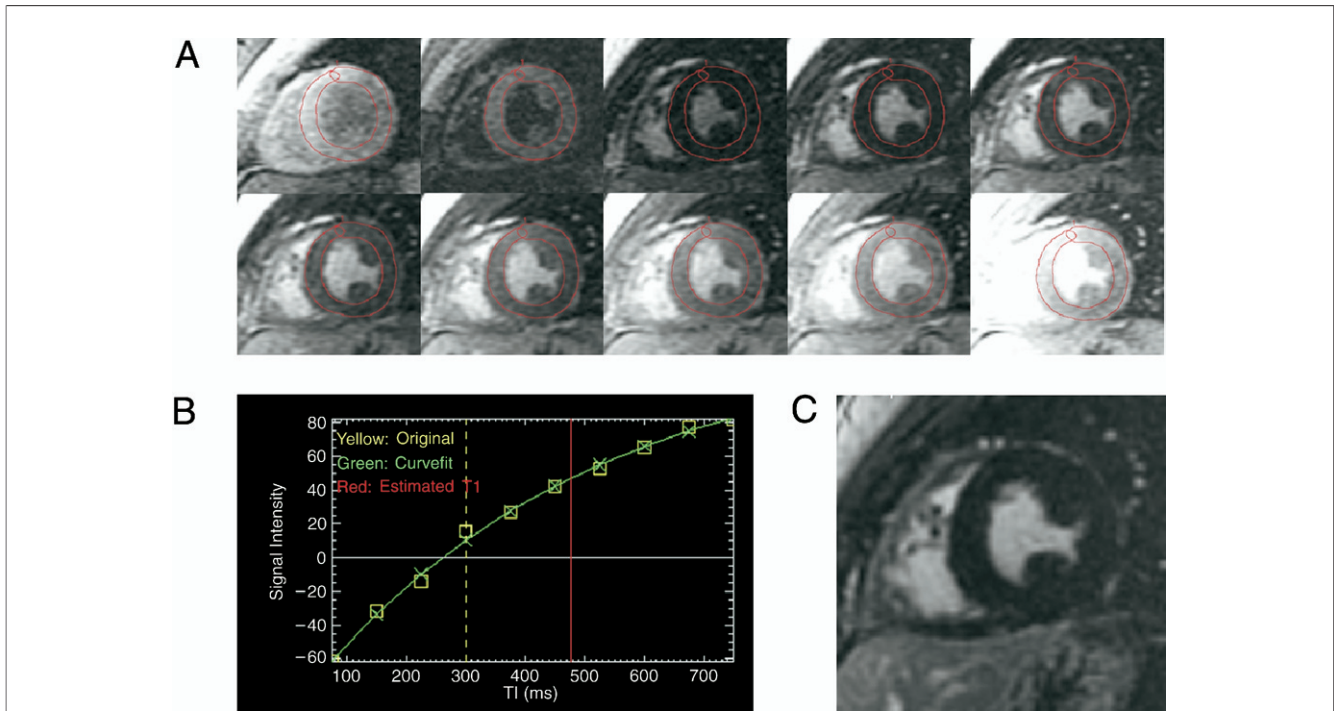


Figure 1 Calculating Myocardial T_1 Time

A region of interest (ROI) was drawn around the left ventricular myocardium in the 10 images obtained from our prototype sequence (A). Signal intensities for each ROI were then curve-fitted to an exponential recovery curve to obtain the myocardial T_1 time for each patient (B). Conventional delayed enhancement imaging (C) was used to demonstrate regional fibrosis.

well represented across a range of etiologies, including ischemic cardiomyopathy (ICMP), infiltrative cardiomyopathy, and IDCM. In all subjects CMRI scanning proceeded without complication, with the T_1 mapping protocol successfully completed.

Relationship of post-contrast myocardial T_1 time to myocardial interstitial fibrosis. To assess the correlation between post-contrast myocardial T_1 time and collagen, we evaluated a separate group of post-transplant patients with routine endomyocardial biopsies (Fig. 2). Collagen volume fraction ranged from 1.5% to 13.3% (mean $8.4 \pm 4.3\%$) and post-contrast myocardial T_1 times from 314 to 656 ms

(mean 521.8 ± 38.9 ms). Collagen content progressively increased as post-contrast myocardial T_1 times shortened ($R = -0.7$, $p = 0.03$), as shown in Figure 3.

Global post-contrast myocardial T_1 times in heart failure and control subjects. In subjects with heart failure, post-contrast myocardial T_1 time was significantly shorter compared with that in control subjects (383 ± 17 ms in heart failure vs. 564 ± 23 ms in control subjects, $p < 0.0001$). This difference remained highly significant when an aged-matched cohort of the control group ($n = 10$) was compared with heart failure subjects (383 ± 17 ms in heart failure vs. 543 ± 32 ms in control subjects, $p < 0.0001$). Slower myocardial clearance of contrast in heart failure due to reduced cardiac output is unlikely to account for this difference, as there was no significant difference in post-contrast skeletal muscle T_1 time between heart failure and control subjects (564 ± 55 ms vs. 521 ± 27 ms, respectively, $p = \text{NS}$). There was also no difference in left ventricular blood pool post-contrast T_1 time between heart failure and control subjects (272 ± 12 ms in heart failure vs. 286 ± 7 ms in control subjects, $p = \text{NS}$). In addition, in control and heart failure subjects there was no correlation between heart rate and post-contrast myocardial T_1 time ($R = 0.14$, $p = \text{NS}$). Prior to contrast administration, there was no difference in myocardial T_1 time between heart failure and control subjects (874 ± 74 ms vs. 975 ± 62 ms, respectively, $p = \text{NS}$).

Table 1 Patient Demographics

	CCF (n = 25)	Control (n = 20)	p Value
Age (yrs)	54 ± 2.2	38 ± 3.0	0.0001
Male, n (%)	18 (72)	10 (50)	NS
Left ventricular ejection fraction (%)	35 ± 3.3	66 ± 1.4	<0.0001
NYHA functional class	2.4 ± 0.1	1.0 ± 0	<0.0001
Heart rate (beats/min)	70 ± 3.4	67 ± 2.4	NS
Heart failure etiology, n (%)			
Ischemic cardiomyopathy	9 (36)	—	—
Idiopathic dilated cardiomyopathy	7 (28)	—	—
Restrictive/infiltrative	9 (36)	—	—

Values expressed as mean \pm standard error unless otherwise specified.
CCF = congestive cardiac failure; NYHA = New York Heart Association.

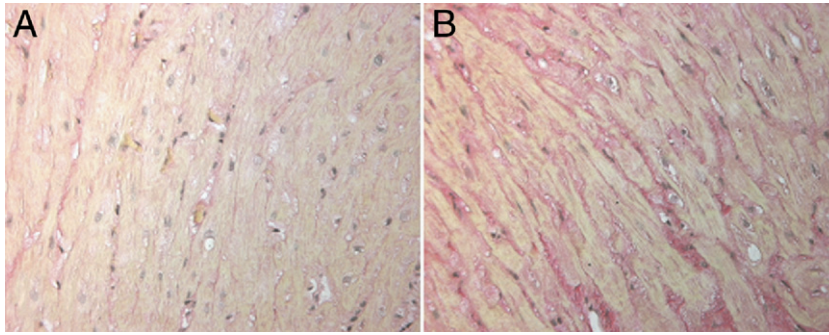


Figure 2 Histologic Findings

Endomyocardial tissue from 2 patients showing minimal (A) and more extensive (B) interstitial fibrosis. Sections were stained with picrosirius red with collagen identified in red and myocytes appearing yellow.

Impact of regional fibrosis on post-contrast myocardial T_1 time. As expected, all 9 subjects with ischemic cardiomyopathy had areas of delayed enhancement on post-contrast CMRI corresponding to regional fibrosis. Over half of all subjects with nonischemic cardiomyopathy also had regional fibrosis, with 5 of 7 subjects with IDCM, and 4 of 9 subjects with infiltrative cardiomyopathy demonstrating delayed enhancement on post-contrast CMRI. Because the presence of regional scarring will clearly affect global post-contrast myocardial T_1 time, we further evaluated the subgroup of subjects with heart failure who had visible regions of delayed enhancement on post-contrast CMRI. In these subjects, the myocardium was subdivided into two areas: myocardium with and without delayed enhancement

(DE+ and DE-, respectively). Separate post-contrast T_1 recovery curves were then constructed in both DE+ and DE- myocardium to separate the effect of regional fibrosis from global post-contrast T_1 time.

Even in DE- areas of myocardium, there was a marked difference in post-contrast myocardial T_1 time between heart failure and control subjects (429 ± 22 ms in heart failure subjects vs. 564 ± 23 ms in control subjects, $p < 0.0001$) (Fig. 4). As expected, there was also a difference in post-contrast T_1 time between DE+ and DE- myocardium in heart failure subjects (333 ± 30 ms in DE+ areas vs. 429 ± 22 ms in DE- areas, $p = 0.02$) (Fig. 4), consistent with a higher degree of fibrosis in regions of myocardium displaying delayed contrast enhancement.

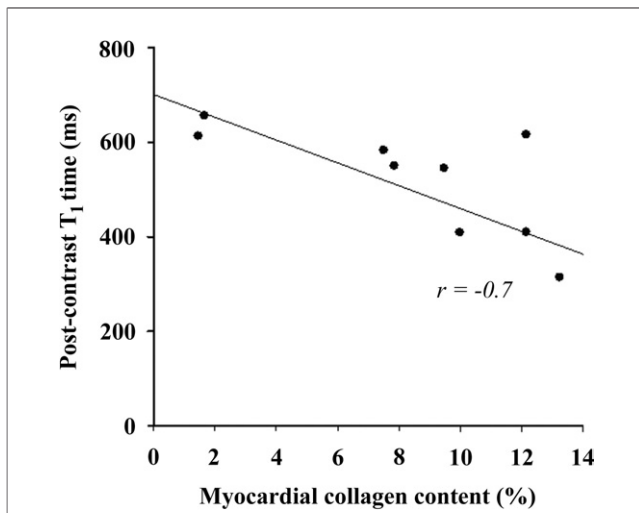


Figure 3 Myocardial Collagen Content and Post-Contrast T_1 Times

Endomyocardial biopsy specimens from 9 subjects after cardiac transplantation were stained with picrosirius red, and collagen content was calculated as a percentage of total myocardial tissue. The post-contrast myocardial T_1 time shortened significantly as the myocardial collagen content increased ($r = -0.7$, $p = 0.03$).

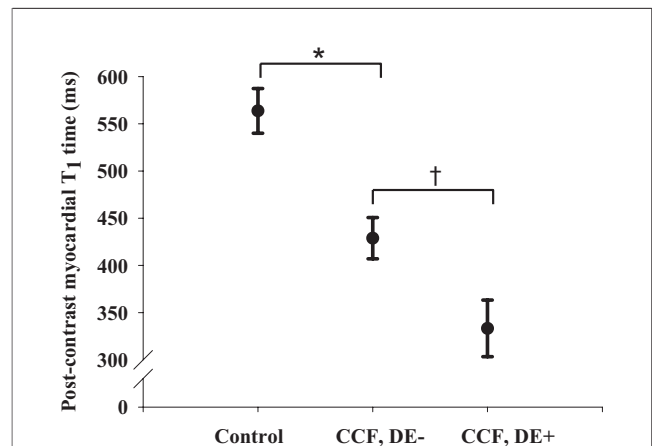


Figure 4 Post-Contrast Myocardial T_1 Times

The myocardium of subjects with heart failure (congestive cardiac failure [CCF]) and regional fibrosis detected by conventional delayed contrast-enhanced imaging was divided into areas with (DE+) and without (DE-) regional scarring. The post-contrast myocardial T_1 time was significantly shorter in DE- regions compared with controls, consistent with diffuse fibrosis even in areas of myocardium not displaying regional scarring ($*p < 0.0001$). There was also a difference in the post-contrast myocardial T_1 time of heart failure subjects between DE- and DE+ areas of myocardium ($\dagger p = 0.02$).

Relationship of post-contrast myocardial T_1 time to systolic and diastolic function. Because diffuse fibrosis may contribute to diastolic dysfunction at a mechanistic level via increased myocardial stiffness, we evaluated the relationship of post-contrast myocardial T_1 time to conventional echocardiographic assessment of LV diastolic function. When diastolic function was graded as normal, impaired, or restrictive there was progressive shortening of the post-contrast myocardial T_1 time (562 ± 24 ms in normal diastolic function vs. 423 ± 33 ms in impaired diastolic function vs. 368 ± 20 ms in restrictive function, $p < 0.001$ by ANOVA), consistent with worsening of diffuse fibrosis across diastolic function grades (Fig. 5). Post hoc analysis revealed a significant difference in post-contrast myocardial T_1 time between normal and both impaired relaxation ($p = 0.03$) and restrictive groups ($p = 0.02$), as well as a strong trend to a difference between impaired and restrictive diastolic function ($p = 0.05$).

As expected, global systolic function and systolic thickening were significantly reduced in heart failure subjects compared with control subjects (left ventricular ejection fraction $35 \pm 3\%$ in heart failure subjects vs. $66 \pm 1\%$ in control subjects, systolic thickening $38 \pm 4\%$ in heart failure subjects vs. $79 \pm 4\%$ in control subjects, $p < 0.0001$ for both). However, we found no correlation between the degree of fibrosis measured by the post-contrast myocardial T_1 time and systolic thickening ($R = 0.32$, $p = \text{NS}$). Finally, because progressive fibrosis has been implicated in adverse remodeling in ischemic cardiomyopathy, we evaluated the impact of diffuse fibrosis in DE– regions of the 9 subjects with heart failure due to ICM. In these subjects, systolic thickening was significantly reduced in noninfarcted segments compared with that in control subjects ($36 \pm 6\%$ vs. $79 \pm 4\%$, $p < 0.0001$), consistent with adverse cardiac remodeling of “healthy” myocardium as an important component of disease progression in ICM.

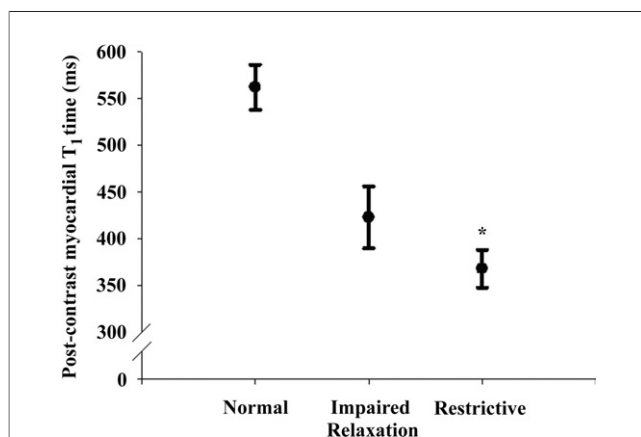


Figure 5 Diastolic Function and Myocardial T_1 Times

Post-contrast myocardial T_1 time progressively shortened with worsening grades of diastolic function (* $p < 0.001$, analysis of variance).

Discussion

Our data demonstrated profound differences in myocardial contrast accumulation between normal and heart failure subjects utilizing post-contrast T_1 mapping, with histologic data supporting our assertion that these changes reflect diffuse fibrosis. These differences remained in age-matched groups, suggesting our findings are not explained by increasing fibrosis with age. The differences also correlated with echocardiographic measurements of diastolic function, indicating shortening of T_1 time may reflect altered diastology as a functional consequence of myocardial fibrosis.

Interestingly, marked changes in myocardial post-contrast T_1 time were observed in heart failure subjects even when the analysis was limited to areas of myocardium without delayed contrast enhancement. This underscores the importance of calculating the myocardial post-contrast T_1 value in such instances, as diffusely fibrotic myocardium may accumulate contrast not detectable by conventional delayed enhanced CMRI. In addition, noninfarcted areas of myocardium in patients with ICM also demonstrated reduced systolic thickening, suggesting pathologic remodeling and fibrosis in these areas. Although pathologic remodeling has been proposed as an important feature in the progression of all types of cardiomyopathy (24–26), our data provide a method of monitoring its progression that could easily be used to evaluate and/or select future therapies aimed at its regression.

A number of limitations should be kept in mind when interpreting our data. This is a small population with heterogeneous causes of heart failure. Gadolinium-based contrast has been shown to accumulate in the myocardium in a number of conditions apart from heart failure, such as arrhythmogenic right ventricular dysplasia, sarcoidosis, and amyloidosis. But in these conditions, delayed enhancement is also thought to be due to the presence of fibrous tissue in fibrofatty change, fibrotic reaction to granulomata, or amyloid deposition, respectively. Contrast accumulation has also been demonstrated in acute myocarditis and infarction, presumably due to local tissue and capillary destruction, with resultant slow clearance of contrast. Altered volume of distribution in infarcted myocardium, due to loss of cellular integrity, is a major element affecting gadolinium-based contrast accumulation. Our study did not include patients with recent infarction or myocarditis, so although caution should be used in applying our data to these patient groups, this is unlikely to account for the changes we observed in our study population.

A number of factors may influence gadolinium-DTPA kinetics. There was no significant difference in renal function between the control and heart failure groups, making impaired clearance an unlikely contributing factor. Although gadolinium-DTPA kinetics and volume of distribution may be altered in heart failure independent of renal function, skeletal muscle and left ventricular blood pool serve as useful internal controls. Indeed, available data on

skeletal muscle changes in heart failure suggest both reduced perfusion (27) and increasing fibrosis (28), both of which would result in impaired clearance of gadolinium-based contrast and therefore, shorter T_1 times of skeletal muscle in heart failure. The fact that we did not observe contrast accumulation in skeletal muscle in heart failure even though significant accumulation occurred in the heart is consistent with a disproportionate amount of myocardial fibrosis. There was also no difference in left ventricular blood pool post-contrast T_1 time between heart failure and control subjects. Finally, variations in heart rate may affect measurement of myocardial T_1 time. In our study, mean heart rate did not differ between heart failure and control groups, and there was no correlation between heart rate and post-contrast myocardial T_1 time in study subjects, excluding heart rate as a significant confounder of our observations.

Conclusions

Cardiac failure is a major cause of morbidity and mortality worldwide. The future challenge to scientists and clinicians alike is to gain a greater understanding of the underlying disease processes to enable development of newer therapies aimed at impeding or reversing disease progression. CMRI T_1 mapping is a promising modality for noninvasive evaluation of diffuse myocardial fibrosis in heart failure, providing important mechanistic insights into the relationship between myocardial fibrosis and diastolic dysfunction. Development of CMRI as a noninvasive tool for evaluating myocardial fibrosis in patients with cardiomyopathy will further our understanding of the underlying physiology and clinical course of heart failure.

Reprint requests and correspondence: Dr. Andrew J. Taylor, Alfred Hospital and Baker IDI Heart and Diabetes Institute, Heart Centre, Alfred Hospital, Commercial Road, Melbourne 3004, Australia. E-mail: andrew.taylor@bakeridi.edu.au.

REFERENCES

1. Koelling TM, Chen RS, Lubwama RN, L'Italien GJ, Eagle KA. The expanding national burden of heart failure in the United States: the influence of heart failure in women. *Am Heart J* 2004;147:74–8.
2. Mann DL. Mechanisms and models in heart failure: A combinatorial approach. *Circulation* 1999;100:999–1008.
3. Kass DA. Ventricular resynchronization: pathophysiology and identification of responders. *Rev Cardiovasc Med* 2003;4 Suppl 2:S3–13.
4. Conrad CH, Brooks WW, Hayes JA, Sen S, Robinson KG, Bing OH. Myocardial fibrosis and stiffness with hypertrophy and heart failure in the spontaneously hypertensive rat. *Circulation* 1995;91:161–70.
5. Kass DA, Bronzwaer JGF, Paulus WJ. What mechanisms underlie diastolic dysfunction in heart failure? *Circ Res* 2004;94:1533–42.
6. Martos R, Baugh J, Ledwidge M, et al. Diastolic heart failure: evidence of increased myocardial collagen turnover linked to diastolic dysfunction. *Circulation* 2007;115:888–95.
7. Sun Y, Weber KT. Cardiac remodeling by fibrous tissue: role of local factors and circulating hormones. *Ann Med* 1998;30 Suppl 1:3–8.
8. Maisch B. Ventricular remodeling. *Cardiology* 1996;87 Suppl 1:2–10.
9. Heling A, Zimmermann R, Kostin S, et al. Increased expression of cytoskeletal, linkage, and extracellular proteins in failing human myocardium. *Circ Res* 2000;86:846–53.
10. The SOLVD Investigators. Effect of enalapril on survival in patients with reduced left ventricular ejection fractions and congestive heart failure. *N Engl J Med* 1991;325:293–302.
11. Diez J, Querejeta R, Lopez B, Gonzalez A, Larman M, Martinez Ubago JL. Losartan-dependent regression of myocardial fibrosis is associated with reduction of left ventricular chamber stiffness in hypertensive patients. *Circulation* 2002;105:2512–7.
12. Pfeffer MA, Swedberg K, Granger CB, et al. Effects of candesartan on mortality and morbidity in patients with chronic heart failure: the CHARM-Overall programme. *Lancet* 2003;362:759–66.
13. Effectiveness of spironolactone added to an angiotensin-converting enzyme inhibitor and a loop diuretic for severe chronic congestive heart failure (the Randomized Aldactone Evaluation Study [RALES]). *Am J Cardiol* 1996;78:902–7.
14. Kim RJ, Wu E, Rafael A, et al. The use of contrast-enhanced magnetic resonance imaging to identify reversible myocardial dysfunction. *N Engl J Med* 2000;343:1445–53.
15. Kim RJ, Fieno DS, Parrish TB, et al. Relationship of MRI delayed contrast enhancement to irreversible injury, infarct age, and contractile function. *Circulation* 1999;100:1992–2002.
16. Scholz TD, Fleagle SR, Burns TL, Skorton DJ. Nuclear magnetic resonance relaxometry of the normal heart: relationship between collagen content and relaxation times of the four chambers. *Magn Reson Imaging* 1989;7:643–8.
17. Grover-McKay M, Scholz TD, Burns TL, Skorton DJ. Myocardial collagen concentration and nuclear magnetic resonance relaxation times in the spontaneously hypertensive rat. *Invest Radiol* 1991;26:227–32.
18. Toni R, Boicelli CA, Baldassarri AM. Characterization of human pathological papillary muscles by $^1\text{H-NMR}$ spectroscopic and histologic analysis. *Int J Cardiol* 1986;11:231–4.
19. Kitamura M, Shimizu M, Kita Y, et al. Quantitative evaluation of the rate of myocardial interstitial fibrosis using a personal computer. *Jpn Circ J* 1997;61:781–6.
20. Saranathan M, Rochitte CE, Foo TK. Fast, three-dimensional free-breathing MR imaging of myocardial infarction: a feasibility study. *Magn Reson Med* 2004;51:1055–60.
21. Taylor AJ, Al-Saadi N, Abdel-Aty H, Schulz-Menger J, Messroghli DR, Friedrich MG. Detection of acutely impaired microvascular reperfusion after infarct angioplasty with magnetic resonance imaging. *Circulation* 2004;109:2080–5.
22. Nishimura RA, Tajik AJ. Evaluation of diastolic filling of left ventricle in health and disease: Doppler echocardiography is the clinician's Rosetta Stone. *J Am Coll Cardiol* 1997;30:8–18.
23. Farias CA, Rodriguez L, Garcia MJ, Sun JP, Klein AL, Thomas JD. Assessment of diastolic function by tissue Doppler echocardiography: comparison with standard transmitral and pulmonary venous flow. *J Am Soc Echocardiogr* 1999;12:609–17.
24. Rosen BD, Edvardsen T, Lai S, et al. Left ventricular concentric remodeling is associated with decreased global and regional systolic function: the Multi-Ethnic Study of Atherosclerosis. *Circulation* 2005;112:984–91.
25. Okada H, Takemura G, Kosai K, et al. Postinfarction gene therapy against transforming growth factor-beta signal modulates infarct tissue dynamics and attenuates left ventricular remodeling and heart failure. *Circulation* 2005;111:2430–7.
26. Hikoso S, Yamaguchi O, Higuchi Y, et al. Pressure overload induces cardiac dysfunction and dilation in signal transducer and activator of transcription 6-deficient mice. *Circulation* 2004;110:2631–7.
27. Wilson JR, Mancini DM. Factors contributing to the exercise limitation of heart failure. *J Am Coll Cardiol* 1993;22:93A–8A.
28. Filippatos GS, Kanatselos C, Manolatos DD, et al. Studies on apoptosis and fibrosis in skeletal musculature: a comparison of heart failure patients with and without cardiac cachexia. *Int J Cardiol* 2003;90:107–13.

Key Words: cardiac magnetic resonance imaging ■ fibrosis ■ heart failure ■ cardiomyopathy.